

Temperature-Modulated Water Filtration Using Microgel-Functionalized Hollow-Fiber Membranes**

Daniel Menne, Fee Pitsch, John E. Wong, Andrij Pich, and Matthias Wessling*

Abstract: In the present work, we investigate the potential of aqueous polymer microgels in membrane technology, especially for filtration applications. The poly(*N*-vinylcaprolactam)-based microgels exhibit thermoresponsive behavior and were employed to coat hollow-fiber membranes used for micro- and ultrafiltration. We discuss the preparation of microgel-modified membranes (by “inside-out” as well as “outside-in” filtration in dead-end mode). The clean-water permeability and stability of these membranes was studied not only as a function of time, but also of temperature. The microgel-modified membranes exhibit a reversible thermoresponsive behavior whereby both the resistance and the retention increased with decreasing temperature.

Modern developments in membrane technology aim to produce interactive membranes with tailored functionality, superior mechanical properties, controlled pore size, switchability, and environmental response for enhanced separation performance. It has recently been shown that hydrogel-modified membranes exhibit less fouling by natural organic matter (NOM) and proteins.^[1,2] Increasing the density of the hydrogel layer results in higher rejection for proteins.^[2,3] Ulbricht and co-workers presented a method to prepare a pore-filled composite membrane based on a track-etched polyethylene terephthalate (PET) membrane.^[4] Their composite membranes were produced by in situ photopolymerization of poly(*N*-isopropylacrylamide) (PNIPAAm) microgels. The membranes showed a reversible temperature-dependent permeability and rejection. La et al. produced

hydrogel-coated membranes for water purification by photopolymerization of poly(ethylene glycol) diacrylate (PEGDA) and a functional monomer containing an ammonium salt (RNH₃Cl).^[5] They observed less fouling during the filtration of bovine serum albumin (BSA) due to surface hydrophilization and antimicrobial activity against *E. coli*. Li and D’Emanuele immobilized thermoresponsive hydrogels on a sintered glass filter with a nominal pore diameter of 20 nm.^[6] They synthesized PNIPAAm microgels within the pores of the glass plate and observed temperature-dependent retention behavior for salicylic acid and BSA through the composite membrane. However, these membrane modifications with hydrogels involve complicated chemical processes such as photo-initiated “grafting from” polymerization.^[1–7]

An alternative and relatively simple route would involve postfunctionalization of the membrane to tune its properties. Plasma treatment^[8,9] and layer-by-layer (LbL) techniques based on the electrostatically driven adsorption of polyelectrolytes,^[10–13] have received great interest. Rana et al. presented recently a systematic review on membrane surface modification to enhance antifouling behavior.^[14]

The straightforward synthesis and high chemical functionality of microgels ensure their use as scavengers,^[15] catalyst supports,^[16] and drug carriers.^[17] Because microgels can also be responsive to environmental changes such as pH, temperature, and light^[18,19] they are gaining more and more interest for applications in membrane separation processes.

In this work we synthesized temperature-responsive microgels based on poly(*N*-vinylcaprolactam) (PVCL)^[20,21] by precipitation polymerization (for detailed information see the Supporting Information). The membranes were modified by was dynamic adsorption,^[22,23] whereby the microgel suspension is filtered through the membrane. The open questions are: a) Can the microgel stay in/on the membrane (pore) surface after modification and under filtration conditions, meaning under convective flow within the membrane pore, and will they remain there even during backwashing. b) Can the microgel retain its thermoresponsive behavior when confined to the surface or within the pores of the membrane? c) Does the switching behavior of the microgel membrane depend on the modification procedure?

In contrast to the other above-mentioned studies on hydrogel/microgel membranes, we are the first to produce microgel-functionalized membranes based on commercially available hollow-fiber membranes that are actually used for water treatment. The applicability for almost all types of membranes (irrespective of geometry and material) and the simplicity of the membrane modification is the main advantage of the method presented in this paper. In addition, the individual properties of the microgel and the membrane can

[*] D. Menne, F. Pitsch, Dr. J. E. Wong, Prof. M. Wessling
Chemical Process Engineering, RWTH Aachen University
Turmstrasse 46, 52064 Aachen (Germany)
E-mail: manuscripts.cvt@avt.rwth-aachen.de
Homepage: <http://www.avt.rwth-aachen.de>

Dr. J. E. Wong, Prof. A. Pich
Functional and Interactive Polymers
Institute of Technical and Macromolecular Chemistry
RWTH Aachen University
Forckenbeckstrasse 50, 52074 Aachen (Germany)
Prof. A. Pich, Prof. M. Wessling
DWI – Leibniz Institute for Interactive Materials
Forckenbeckstrasse 50, 52074 Aachen (Germany)

[**] We thank the German Research Foundation (DFG) SFB 985
“Functional Microgels and Microgel Systems”, the Alexander-von-Humboldt Foundation (M.W.), and the Volkswagen Foundation (A.P.) for financial support.

Supporting information for this article (including details concerning setups, membranes, chemicals, and the synthesis and characterization of microgels and membranes) is available on the WWW under <http://dx.doi.org/10.1002/anie.201400316>.

be fine-tuned independently to further optimize the performance of the resulting microgel-functionalized membrane.

Both micro- and ultrafiltration poly(ethersulfone) (PES) hollow-fiber membranes employed exhibit an asymmetric pore structure with pore dimensions of 30 nm for the ultrafiltration membrane and 200 nm for the microfiltration membrane on the lumen (inner) side and a few microns on the shell (outer) side. Due to this asymmetry two distinct dynamic coating procedures were adopted: an “inside-out” and an “outside-in” coating, both performed at constant flux of $30 \text{ L m}^{-2} \text{ h}^{-1}$ (LMH) and at $T=23^\circ\text{C}$, that is, when the microgels are in the swollen state.

The graphs in this section depict either the transmembrane pressure (TMP) or the membrane's resistance. The resistance is defined by Equation (1), where Δp is the TMP, η is the viscosity, and J is the flux. Due to the change of the viscosity with the temperature, the plotted resistance is temperature-corrected and thus can be used to compare directly the performance of the membrane at different temperatures.

$$R = \frac{\Delta p}{\eta J} \quad (1)$$

The microgel-modified membranes were prepared by dynamic adsorption at a constant flux of 30 LMH. During the adsorption the microgels are transported convectively to the membrane surface where they finally are retained by size exclusion or adsorption. The retained microgels build up an additional filtration resistance leading to a TMP increase (Figure 1). This additional resistance will differ locally and thus the flux will be influenced as well. The flux will be locally increased at positions of lower resistance. Due to the increased flux at those positions the convective transport of microgels towards the surface will be greater as well. This explains why the slope of the TMP plot increases with time.

The deposition of the microgels was stopped when a maximum TMP of bar is reached; this value is reached earlier for the “inside-out” than for the “outside-in” coating (Figure 1). The outer surface is greater than the lumen surface and therefore the complete adsorption takes a longer time for the “outside-in” coating. In addition, due to the asymmetric nature of the hollow-fiber membrane, the lumen surface is denser than the shell surface with pore size much bigger than the microgel particles. During an “outside-in” coating the microgels are not only deposited and adsorbed on the shell surface, but they are also transported 2–3 μm into the porous structure (Figure 2a and b). Since microgels are soft and deformable particles, their penetration depth into the membrane pores will be influenced not only by the hydrodynamic radius (r_h) of the microgels, but also by the stiffness determined by the cross-linking density.^[24] On the lumen side of the “outside-in”-coated membrane no microgels could be found neither on the surface, nor within the dense porous structure of the inner side (Figure 2c and d) showing that the microgels do not penetrate through the complete membrane. For the “inside-out”-coated membrane we observed no microgels on the shell side but only on the surface of the membrane lumen (Figure 2e and f).

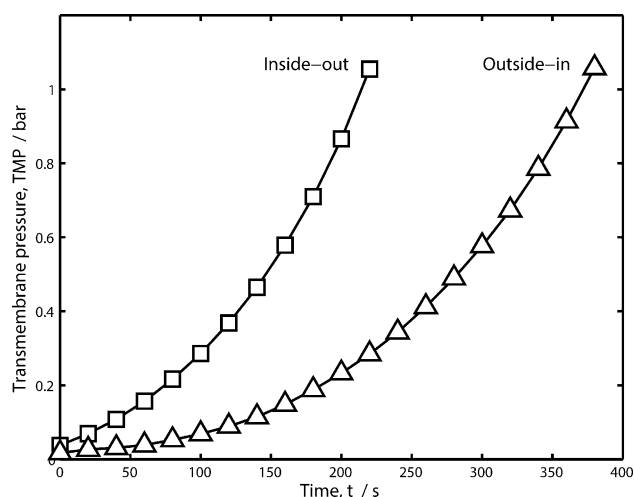


Figure 1. Transmembrane pressure (TMP) as a function of time during microgel coating at constant flux of $30 \text{ L m}^{-2} \text{ h}^{-1}$ (LMH), \square : “inside-out”-coated membrane, \triangle : “outside-in”-coated membrane.

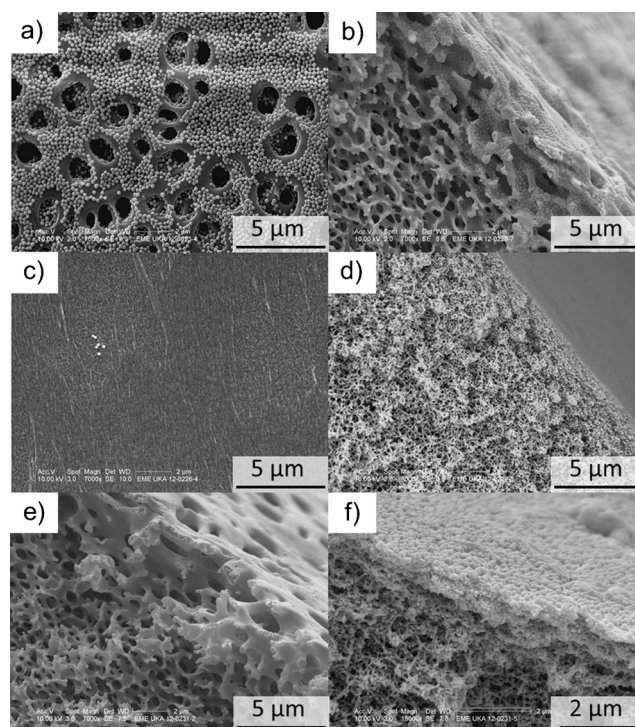


Figure 2. SEM images of microgel membranes: a) “outside-in”-modified/shell side, b) “outside-in”-modified/outer cross section, c) “outside-in”-modified/lumen side, d) “outside-in”-modified/inner cross section, e) “inside-out”-modified/outer cross section, f) “inside-out”-modified/inner cross section.

The SEM images in Figure 2a–f distinguish between two distinct coating procedures: a) A microgel coating on the active layer, meaning on the membrane lumen side by an “inside-out” filtration and b) a coating of the membrane surface on the shell side as well as pore filling by filtration of the microgels from the outside to the inside.

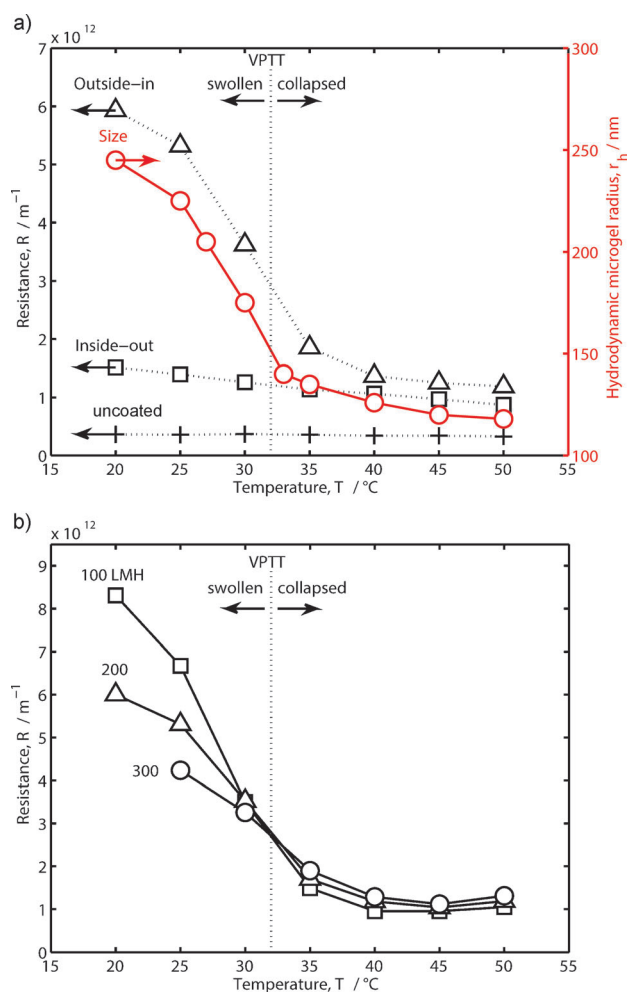


Figure 3. a) Membrane resistance (left y-axis) and microgel size (right y-axis) as a function of temperature; Δ : “outside-in”-coated membrane, \square : “inside-out”-coated membrane, $+$: uncoated membrane, \circ : hydrodynamic radius of microgel, determined by dynamic light scattering. b) Membrane resistance as a function of temperature for varied flux of an “outside-in”-modified membrane, \square : 100 LMH, Δ : 200 LMH, \circ : 300 LMH.

The membrane’s resistance was investigated as a function of temperature by pure-water filtration at constant flux in dead-end mode (Figure 3a). Hereby the temperature of water was increased in steps of 5 $^{\circ}\text{C}$ from 20 to 50 $^{\circ}\text{C}$. For both types of coatings, “inside-out” as well as “outside-in”, the resistance of the membrane is temperature dependent and decreases to reach a plateau (at $T > 32^{\circ}\text{C}$) which is indicative of the collapsed state of the microgels. In the case of the “outside-in” coating the resistance decreases dramatically around the volume phase-transition temperature (VPTT) of the microgels. Below this temperature carbonyl groups of VCL interact with water molecules forming hydrogen bonds and therefore PVCL chains became well solvated with water molecules. In this situation polymer–water interactions dominate over hydrophobic polymer–polymer interactions. At temperatures above the VPTT destruction of hydrogen bonds occurs and hydrophobic interactions dominate leading to the particle shrinkage. At higher temperatures the microgels integrated in the membrane structure collapse, thereby generating more

accessible volume that facilitates water permeation. This is in line with the decrease of the microgel size as is depicted in Figure 3a. During the “inside-out” coating only the inner surface is coated with swollen microgels. Increasing the temperature also causes the membrane’s resistance to decrease, but the impact is much less than that of the “outside-in”-coated membrane.

The membrane’s resistance as a function of temperature was also investigated at various flux rates (Figure 3b). At temperatures below VPTT the microgel membrane shows lower resistance at higher applied fluxes. A higher flux is achieved by increasing the TMP. Swollen microgels contain 70–80 % water^[25] and are highly deformable. Therefore an increased pressure leads to more accessible volume for water permeation; however, the shear forces exerted are apparently not large enough to cause detachment and washing out of the microgel as will be shown in detail below.

The stability of the microgel membrane is of paramount interest. Therefore several measurements with dead-end filtration alternating with backwashing were performed (Figure 4a). For both the “inside-out”- and the “outside-in”-coated membranes, the microgels could not be removed by backwashing. The resistance before and after the backwash is identical, indicating that no significant amount of microgels was removed. The microgels must be firmly bound by strong adsorption on the surface of the PES membrane. The fuzzy microgel surface and high deformation on solid surfaces ensure the strong adhesion of microgels to different solid substrates.^[26] However, the exact mechanism by which these microgels adhere to the membrane is still not fully understood.

Furthermore the microgel-modified membranes were stored in complete darkness (to minimize bio-fouling and growth of microorganisms) to investigate the long-term stability. Within this extended storage time several pure-water permeability measurements were conducted. Within the first three days the membrane’s resistance decreased rapidly, indicating some loss of microgels in this period. After three days the resistance remained constant. The SEM images (Figure 2) were recorded after the coated-membranes had been stored for 45 days and after several permeability and backwashing experiments had been conducted. It is clear from Figure 2 that the microgels are still present, showing that the prepared membranes are stable over the period studied (about six weeks).

To investigate the reversibility of the membrane’s resistance with switching temperature, the membrane’s resistance was alternatively measured with water at 20 and 45 $^{\circ}\text{C}$ (Figure 4b). For both the “inside-out”- and the “outside-in”-coated membranes we observed that the change of the resistance is completely reversible with the temperature. This is in line with the change of the PVCL microgel’s size, which also behaves completely reversibly with temperature changes.^[27]

The uncoated ultrafiltration membrane retained humic acid almost completely and therefore could not be used to demonstrate and quantify a temperature modulation of the retention behavior. A microfiltration membrane (MF) with similar composition as the ultrafiltration membrane was

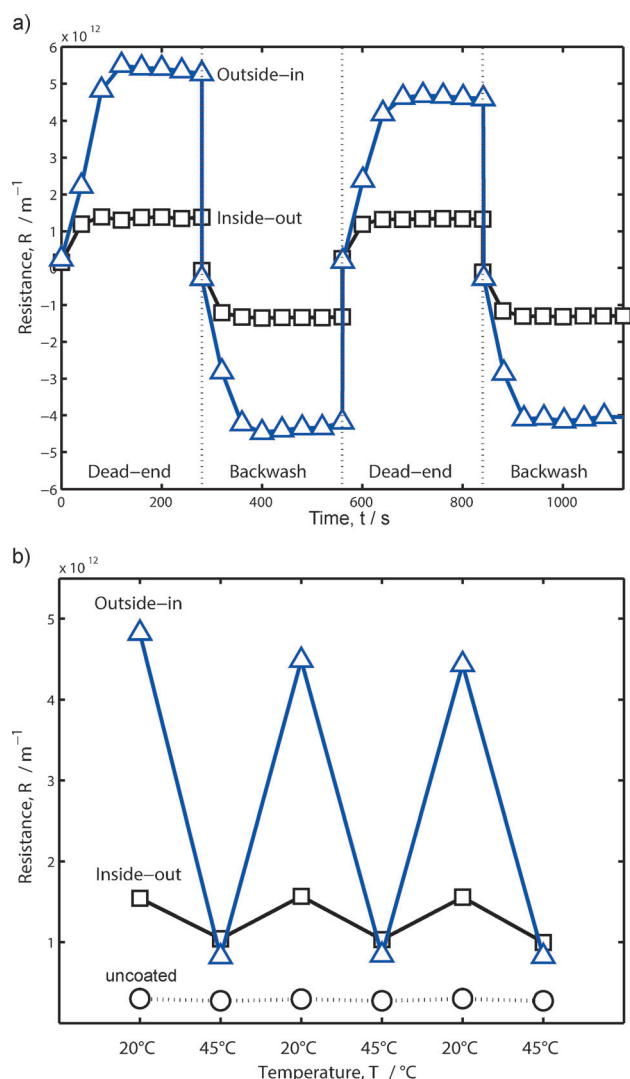


Figure 4. a) Backwash stability determined by constant-flux filtration at 100 LMH: Δ : “outside-in”-coated membrane, \square : “inside-out” coated membrane. b) Microgel membrane stability at alternating temperatures of 20 and 45 °C determined at 100 LMH: Δ : “outside-in”-coated membrane, \square : “inside-out”-coated membrane, and \circ : uncoated membrane.

employed instead which has a retention for humic acid of roughly 40 to 50 %. The microfiltration membrane with an “inside-out” coating of microgels was tested at 25 and 45 °C, and shows similar retention at 45 °C to that of the uncoated MF (Figure 5). However, at 25 °C the retention increased to about 80 % showing the thermoresponsive behavior of the coated MF membrane. A similar effect was observed with the “outside-in”-coated MF membrane; however, these measurements were not as reproducible as the retention tests with the “inside-out”-coated MF membranes.

The experimental data summarized herein demonstrate that modification of conventional hollow-fiber membranes with stimuli-responsive microgels provides a straightforward and versatile route for the design of functional membranes with new properties. The stimuli-responsiveness of the microgels immobilized in the membrane pores is retained and

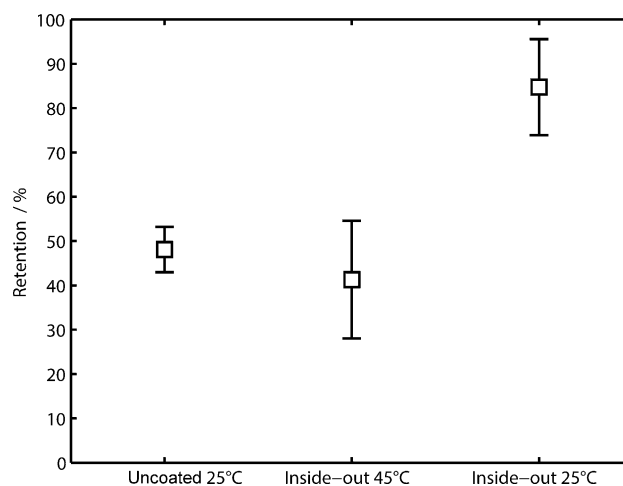


Figure 5. Humic acid retention of uncoated and “inside-out”-coated microfiltration membrane at 25 and 45 °C.

allows the regulation of the flow profile and resistance. Additionally, the chemical structure of microgels provides a toolbox for the incorporation of specific functionalities into membranes, thus increasing the efficiency and selectivity of separation processes. We believe that the proposed method can be developed in the future as a platform technology for the design of interactive membranes for various applications.

Received: January 11, 2014

Published online: April 16, 2014

Keywords: dynamic adsorption · hollow-fiber membranes · thermoresponsive microgels · ultrafiltration membranes

- [1] H. Susanto, M. Ulbricht, *Water Res.* **2008**, *42*, 2827–2835.
- [2] P. D. Peeva, T. Pieper, M. Ulbricht, *J. Membr. Sci.* **2010**, *362*, 560–568.
- [3] P. D. Peeva, N. Million, M. Ulbricht, *J. Membr. Sci.* **2012**, *390*, 99–112.
- [4] N. Adrus, M. Ulbricht, *J. Mater. Chem.* **2012**, *22*, 3088.
- [5] Y.-H. La, B. D. McCloskey, R. Sooriyakumaran, A. Vora, B. Freeman, M. Nassar, J. Hedrick, A. Nelson, R. Allen, *J. Membr. Sci.* **2011**, *372*, 285–291.
- [6] S. K. Li, A. D’Emanuele, *J. Controlled Release* **2001**, *75*, 55–67.
- [7] S. Frost, M. Ulbricht, *J. Membr. Sci.* **2013**, *448*, 1–11.
- [8] M. L. Steen, L. Hymas, E. D. Havey, N. E. Capps, D. G. Castner, E. R. Fisher, *J. Membr. Sci.* **2001**, *188*, 97–114.
- [9] K. S. Kim, K. H. Lee, K. Cho, C. E. Park, *J. Membr. Sci.* **2002**, *199*, 135–145.
- [10] G. Decher, *Science* **1997**, *277*, 1232–1237.
- [11] A. A. Antipov, G. B. Sukhorukov, H. Möhwald, *Langmuir* **2003**, *19*, 2444–2448.
- [12] R. v. Klitzing, B. Tieke, *Adv. Polym. Sci.* **2004**, *165*, 177–210.
- [13] J. Kochan, T. Wintgens, J. E. Wong, T. Melin, *Desalination* **2010**, *250*, 1008–1010.
- [14] D. Rana, T. Matsuura, *Chem. Rev.* **2010**, *110*, 2448–2471.
- [15] S. Berger, R. Singh, J. D. Sudha, H.-J. Adler, A. Pich, *Polymer* **2010**, *51*, 3829–3835.
- [16] Y. Lu, Y. Mei, M. Drechsler, M. Ballauff, *Angew. Chem.* **2006**, *118*, 827–830; *Angew. Chem. Int. Ed.* **2006**, *45*, 813–816.
- [17] A. V. Kabanov, S. V. Vinogradov, *Angew. Chem.* **2009**, *121*, 5524–5536; *Angew. Chem. Int. Ed.* **2009**, *48*, 5418–5429.

- [18] R. Pelton, *Adv. Colloid Interface Sci.* **2000**, 85, 1–33.
 - [19] S. Berger, H. Zhang, A. Pich, *Adv. Funct. Mater.* **2009**, 19, 554–559.
 - [20] V. Boyko, A. Pich, Y. Lu, S. Richter, K.-F. Arndt, H.-J. P. Adler, *Polymer* **2003**, 44, 7821–7827.
 - [21] A. Pich, A. Tessier, V. Boyko, Y. Lu, H.-J. P. Adler, *Macromolecules* **2006**, 39, 7701–7707.
 - [22] G. Zhang, W. Gu, S. Ji, Z. Liu, Y. Peng, Z. Wang, *J. Membr. Sci.* **2006**, 280, 727–733.
 - [23] G. Zhang, H. Yan, S. Ji, Z. Liu, *J. Membr. Sci.* **2007**, 292, 1–8.
 - [24] D. A. Holden, G. R. Hendrickson, W.-J. Lan, L. A. Lyon, H. S. White, *Soft Matter* **2011**, 7, 8035.
 - [25] I. Berndt, W. Richtering, *Macromolecules* **2003**, 36, 8780–8785.
 - [26] J. C. Gaulding, M. W. Spears, L. A. Lyon, *Polym. Chem.* **2013**, 4, 4890.
 - [27] G. Agrawal, J. Wang, B. Bruster, X. Zhu, M. Möller, A. Pich, *Soft Matter* **2013**, 9, 5380.
-